IMECE2005-79902

CONVECTIVE HEAT TRANSFER OF LAMINAR, SINGLE-PHASE FLOW IN RANDOMLY ROUGH MICROTUBES

M. Bahrami,[1] **M. M. Yovanovich,**[2] **and J. R. Culham**[3]
Microelectronics Heat Transfer Laboratory
Department of Mechanical Engineering
University of Waterloo, Waterloo, ON, Canada N2L 3G1

Abstract

Convective heat transfer of laminar, single-phase flow in rough microtubes is studied. Wall roughness and slope are assumed to possess Gaussian, isotropic distributions. Fractal concepts are used to model the rough microtube. It is shown that due to the existence of wall roughness, both cross-sectional and inside surface areas are increased. A new concept is defined as a figure of merit for assessing thermal performance of rough microtubes. As a result of increasing roughness, an enhancement is observed in the thermal performance of microtubes. The present model can be extended to analyze other geometries such as rectangular and trapezoidal microchannels.

Nomenclature

A_c	=	cross-sectional area, m^2
A	=	surface area, m^2
a	=	mean radius of rough microtube, m
c_p	=	fluid specific heat, kJ/kgK
D	=	microtube diameter, m
h	=	convection heat transfer coefficient, W/m^2K
k	=	fluid thermal conductivity, W/mK
L	=	sampling length, m
m_{abs}	=	mean absolute surface slope, $[-]$
$\dot{m}$	=	mass flow rate, kg/s
Nu	=	Nusselt number $\equiv hD/k$
q_w	=	wall heat flux, W/m^2
r	=	local microtube radius, m

T	=	temperature, K
u	=	fluid velocity, m/s
x	=	fluid flow direction

Greek

ϵ	=	relative roughness, σ/a
η	=	non-dimensional radial location $\equiv r/a$
ζ	=	non-dimensional length, x/L
θ	=	surface angle, rad
θ_T	=	non-dimensional temperature
ρ	=	fluid density, kg/m^3
σ	=	roughness standard deviation, m
σ_m	=	slope standard deviation, rad

Subscripts

0	=	smooth microtube
θ	=	in angular direction
m	=	mean value
x	=	in longitudinal direction

---

[1] Post-Doctoral Fellow. Mem. ASME. Corresponding author. E-mail: majid@mhtlab.uwaterloo.ca.
[2] Distinguished Professor Emeritus. Fellow ASME.
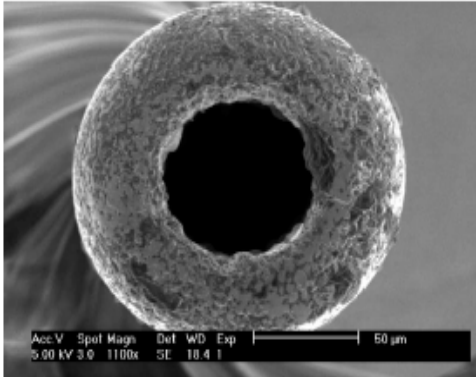[3] Associate Professor and Director of MHTL. Mem. ASME.

1 INTRODUCTION

The flow of liquids through microtubes and microchannels is becoming increasingly important as the size of mechanical devices and biological and chemical sensors continues to shrink. This has led to a series of recent investigations focused on measuring pressure drop and heat transfer rates through microtubes, see survey articles [1; 2; 3].

Microchannels also present a great potential for microelectronics cooling and fuel cell technologies. They can be integrated directly within the heat generating component; thus the thermal contact resistance at the interface

Figure 1. CROSS-SECTION OF A ROUGH MICROTUBE, FROM REF. [6]

Figure 2. MICROTUBE ELEMENT

of a heat-generating component and heat sink is eliminated. This feature leads to lower substrate temperatures and smaller temperature gradients [4].

As the diameter of (micro-) tubes decreases the surface to volume ratio, which is equal to $2/r$, increases rapidly. Consequently, the surface phenomena- including the effect of wall roughness, see Fig. 1, become more significant. The effects of roughness on pressure drop of microtubes have been experimentally investigated by several researchers, to name a few see Li et al. [5; 6; 7]. These studies consistently show an increase in the friction factor due to the surface roughness when compared with the classical, smooth theory. The same authors [8] developed a novel analytical model that predicts the trends of empirically determined friction factors for rough microtubes.

The effects of surface roughness on single-phase convective heat transfer of microchannels have also been experimentally investigated by some researchers. However, unlike the pressure drop data, the reported trends in the heat transfer data are rather inconsistent.

Celata et al. [9] performed heat transfer experiments in capillary tubes with R114 and water with tube diameters ranging from 130 - 290 μm. Microtubes were heated by direct condensation on the outer surface of the tube (isothermal boundary condition was assumed). Celata et al. compared their experimental results with the correlations developed for conventional laminar and turbulent flows. They concluded that the conventional theories were not adequate for predicting heat transfer in microtubes [9]. Kandlikar et al. [10] studied the effect of surface roughness on the local Nusselt number of rough microtubes of radii 1.032 and 0.62 mm. Kandlikar et al. reported an increase in the heat transfer for the microtubes with higher relative roughness $\epsilon \sim 0.01$. The roughness of the inside tube surface was created by etching with an acid solution [10]. Gao et al. [11]
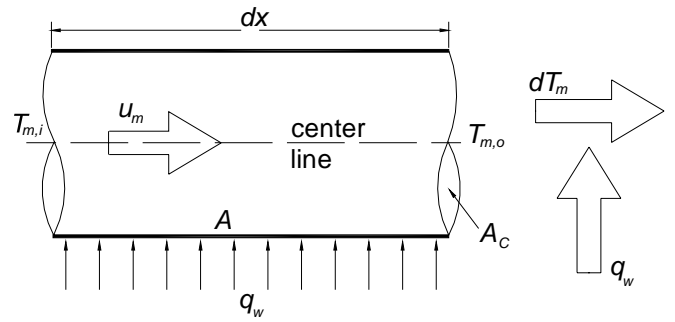
investigated the single-phase heat transfer in two dimensional microchannels. They designed an experimental rig in such a manner that the height of the test microchannel could be changed from 1 to 0.1 mm. Their measured local Nusselt numbers were in good agreement with the conventional theories for larger channel heights. However, at lower values of the channel heights (< 0.4 mm), they encountered a significant decrease in the Nusselt number [11].

As briefly reviewed above, the published data show a significant scatter which may be a result of various conditions used in experiments, and most likely a direct result of the difficulties of thermal measurements at micron levels.

There is a need for a better understanding of the effect of wall roughness on heat transfer characteristics in microchannels and microtubes. No physical model exists in the literature that accounts for the wall roughness effects. The goal of this paper is to develop a predictive model for the convective heat transfer of laminar, single-phase flows in rough microtubes.

2 THERMAL PERFORMANCE OF MICROTUBES

The assumptions of the present model are summarized as:

- the fluid flow is laminar. The fluid is forced to move by a pressure gradient applied to the ends of the microtubes, i.e. pressure-driven flow.
- the fluid is Newtonian and the microtube cross-section is circular.
- the microtube walls are rough; the roughness is assumed to be Gaussian, i.e., isotropic. Also, there are no *macro* deviations or *waviness* inside the microtubes.
- rarefaction, compressibility, and slip-on-wall effects are negligible.
- the entire inside area of the rough microtube is wetted.
- fluid properties are constant.

2

Some researchers have reported that the transition from laminar to turbulent flow regimes starts at lower Reynolds numbers in microchannels. However, this early transition has not been observed by Judy et al. [6]. Also Obot [12] presented a critical review of published data and concluded that there is hardly any evidence to support the occurrence of transition of turbulence in smooth microchannels for Re < 1000. Therefore, the focus of this study is on the laminar flow regime.

A new parameter (dT_m/dx), change in the fluid mean temperature over the tube length, is defined as a figure of merit to assess the thermal performance of randomly rough microtubes.

Consider a microchannel of inside surface area dA, cross-sectional area A_c, and length dx where the mean velocity of the fluid is u_m, as shown in Fig. 2. The mean temperatures at the inlet and the exit of the element are $T_{m,i}$ and $T_{m,o}$ also a uniform wall heat flux q_w can be assumed for an element. Applying an energy balance for an element dx, one can write

$$\rho \, c_p \, A_c \, u_m \, dT_m = q_w \, dA \qquad (1)$$

Equation (1) is general, i.e., it is not limited to any specific thermal boundary condition. It is also valid for both developing and fully-developed regions. The mean velocity u_m and the mean temperature T_m are defined as [13]:

$$u_m = \frac{\int_{A_c} \rho u \, dA_c}{\rho A_c}$$

$$T_m = \frac{\int_{A_c} \rho u c_p T \, dA_c}{\dot{m} c_p}$$

where $\dot{m}$ is the mass flow rate. Equation (1) can be rearranged as

$$\frac{dT_m}{dx} = \frac{2q_w \, A^*}{\rho \, c_p a \, u_m A_c^*} \qquad (2)$$

where $A^* = dA/dA_0$, $A_c^* = A_c/A_{c,0}$, $dA_0 = 2\pi a dx$, and $A_{c,0} = \pi a^2$. Subscript 0 denotes the smooth microtube and a is the mean statistical average of the local radius over the entire microtube.

In the following sections, relationships for the surface area and cross-sectional area of rough microtubes are derived. Implementing the same approach, the present model can be extended to other geometries such as rectangular and trapezoidal microchannels. A brief introduction on roughness is presented in the next section.

3 ROUGHNESS

Roughness or surface texture can be thought of as the surface deviation from its nominal topography. The term

Gaussian is used to describe a surface where its asperities are isotropic and randomly distributed over the surface.

Five types of instruments are currently available for measuring the surface topography [14]: i) stylus-type surface profilometer, ii) optical (white-light interference) measurements, iii) Scanning Electron Microscope (SEM), iv) Atomic Force Microscope (AFM), and v) Scanning Tunneling Microscope (STM). Among these, the first two instruments are usually used for macro-to-macro asperity measurements, whereas the others may be used for micro or nanometric measurements. Surface texture is most commonly measured by a profilometer, which draws a stylus over a sample length of the surface. A datum or centerline is established by finding the straight line, or circular arc in the case of round components, from which the mean square deviation is a minimum. Some of the rough surface characteristics are:

$$R_a = \frac{1}{L} \int_0^L |z(x)| \, dx \qquad (3)$$

where L is the sampling length in the x direction and $z(x)$ is the measured value of the surface heights along this length. When the surface is Gaussian, the standard deviation σ is identical to the RMS value [15], R_q

$$\sigma = R_q = \sqrt{\frac{1}{L} \int_0^L z^2(x) \, dx} \qquad (4)$$

For a Gaussian surface, Ling [16] showed that the average and RMS values are related as, $R_q \approx \sqrt{\pi/2} R_a \approx 1.25 R_a$. Similarly, the absolute average and RMS asperity slopes, m_{abs} and σ_m respectively, can be determined across the sampling length from the following:

$$m_{abs} = \frac{1}{L} \int_0^L \left| \frac{dz(x)}{dx} \right| \, dx \qquad (5)$$

$$\sigma_m = \sqrt{\frac{1}{L} \int_0^L \left(\frac{dz(x)}{dx} \right)^2 \, dx}$$

Mikic and Rohsenow [17] showed that for Gaussian surfaces the relationship between the average and RMS values of the asperity slopes is $\sigma_m \approx 1.25 m_{abs}$.

4 ROUGH MICROTUBES

Consider a rough microtube with the mean radius a and length dx as shown schematically in Fig. 3. The wall roughness of the microtube is assumed to posses a Gaussian distribution in the angular direction. Owing to the random nature of the wall roughness, an exact value of the local
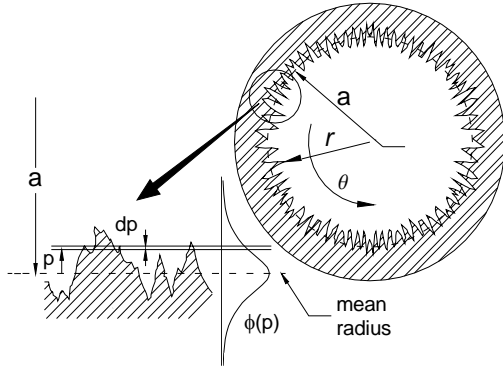
Figure 3. CROSS-SECTION OF A MICROTUBE: WALL ROUGHNESS AND GAUSSIAN DISTRIBUTION

Figure 4. LONGITUDINAL CROSS-SECTION OF RANDOM ROUGH MICROTUBE

radius, r, can not be specified. Instead, probabilities of occurring different radii should be computed. A random variable, p, is used to represent the deviations of the local radius, r, in the angular direction, Fig. 3. The standard deviation of p is the wall roughness σ_θ and has the following Gaussian distribution:

$$\phi\left(p\right) = \frac{1}{\sqrt{2\pi}\sigma_\theta}\exp\left(-\frac{p^2}{2\,\sigma_\theta^2}\right) \quad (6)$$

The local radius can vary over a wide range of values from much larger to much smaller radii than the mean radius a, valleys and hills in the figure, with the Gaussian probability distribution shown in Eq. (6). The microtube wall also has roughness in the longitudinal direction x, see Fig. 4. The variations of the local radius of the microtube, r, in the longitudinal direction is presented by another random variable q, with the same Gaussian distribution as in the angular direction.

$$\phi\left(q\right) = \frac{1}{\sqrt{2\pi}\sigma_x}\exp\left(-\frac{q^2}{2\,\sigma_x^2}\right) \quad (7)$$

The local radius of the microtube can be written as

$$r = a + p + q \quad (8)$$

where a is the mean statistical value of the local radius, r, over the cross-sections over the entire length, dx, of the microtube.

To better understand Eq. (8), consider cross-sections of a rough microtube at different longitudinal locations, Fig. 4. These cross-sections have different mean radii where the probability of these radii occurring can be determined from Eq. (7), $a + q$. Meanwhile, the actual radius at each cross-section varies around the mean radius, $a + q$, in the angular direction (variations of p) with the probability distribution
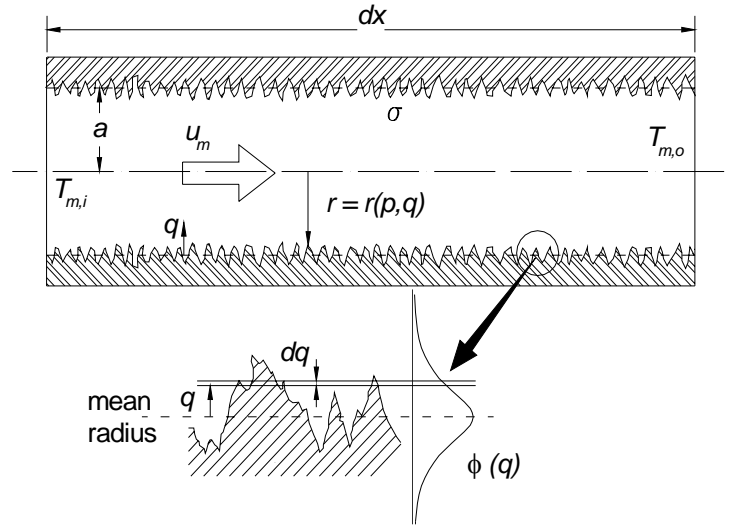
described in Eq. (6). Therefore, the local radius of a microtube, r, is a function of both random variables p and q, i.e. $r = r(p,q)$. We assume that the local radius is the superposition of the two random variables, as shown in Eq. (8). Note that the variables p and q are independent. For argument sake, consider an imaginary case where a microtube has roughness only in the angular direction; thus one can write, $r = r(p)$. As a result, an average of these variables $[r = a + (p + q)/2]$ is not a correct radius.

In the general case, the standard deviations σ_θ and σ_x might be different. However, in this study, we assume an isotropic roughness, i.e., $\sigma_\theta = \sigma_x = \sigma$.

4.1 Cross-Sectional Area, $\mathbf{A}_c$

The cross-sectional area of a rough microtube is calculated from, $A_c = \pi r^2$. Using Eq. (8), it can be written

$$A_c = \pi \int_{-\infty}^{+\infty} \int_{-\infty}^{+\infty} \left(a + p + q\right)^2 \phi\left(p\right)\phi\left(q\right) dp\,dq \quad (9)$$

Equation (9) considers the probabilities of all values of radius, r, occurring according to the Gaussian distribution. It should be noted that it is mathematically possible for the variables p and q to have values ranging from $-\infty$ to $+\infty$, see Eqs. (6) and (7). However, the probability of occurring much larger/ smaller radii than the mean radius, a, are quite small.

After changing variables and simplifying, Eq. (9) be-

4

comes

$$A_c^* = \frac{1}{2\pi} \int_{-\infty}^{+\infty} \int_{-\infty}^{+\infty} (1 + \epsilon u + \epsilon v)^2 \, e^{-u^2/2} e^{-v^2/2} du \, dv \tag{10}$$

where ϵ is the relative surface roughness

$$\epsilon = \frac{\sigma}{a} \tag{11}$$

Note that the relative roughness, ϵ, is defined as the RMS surface roughness over the *radius* of the microtube. Equation (10) calculates an *effective* cross-sectional area for rough microtubes. After solving the integral, one finds

$$A_c^* = \frac{A_c}{A_{c,0}} = 1 + 2\epsilon^2 \tag{12}$$

As expected, the effect of surface roughness is to increase the cross-sectional area of a rough tube. Notice that at the limit where roughness goes to zero $\epsilon \to 0$ (smooth surface), $A_c^* \to 1$.

4.2 Surface Area, A

Surface area increases, compared with the nominal (projected) area, as roughness is increased. This enhancement depends on the process that created the surface and the properties of the surface material.

A unique property of random rough surfaces is that if a surface is repeatedly magnified, increasing details of roughness are observed right down to nanoscale. According to Majumdar and Tien [18], the roughness at all magnifications appear quite similar. Microscopic observations have shown that engineering surfaces can be characterized by *fractals* from the nanometer to the millimeter scale [18; 19]. A fractal is a geometrical shape or motif made up of identical parts which are in turn identical to the overall pattern. The term fractal was coined by Benoit Mandelbrot [20] to describe a complex geometrical object that has a high degree of *self-similarity* and a *fractional dimension*. Figure 5 shows an example of fractal geometries of similar equilateral triangles built on different scales with a side angle of θ where n denotes the number of scales.

Mathematically, fractal surfaces are i) continuous, ii) statistically self-similar, and iii) non-differentiable. The non-differentiability arises from the fact that a tangent plane cannot be drawn at any point on the surface since more and more details of roughness will appear at that point. Moreover, fractal dimensions are non-integers which makes the direct implementation of the fractal theory rather complex.

With the fractal concept, a new model is proposed for estimating the real surface area of random rough surfaces.
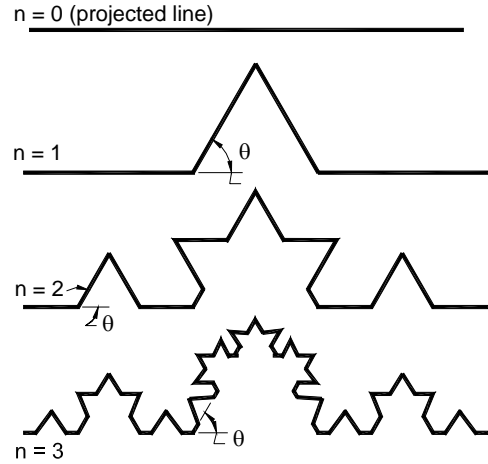

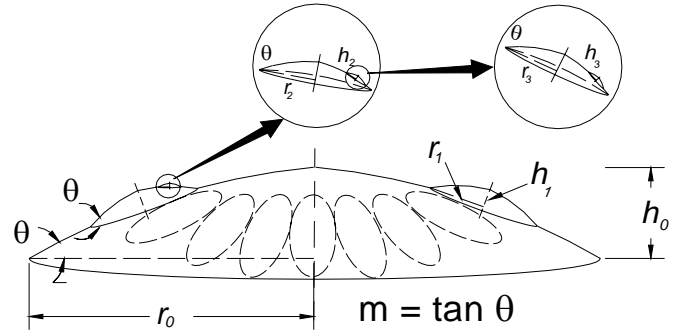Figure 5. FRACTAL GEOMETRIES ARE SIMILIAR AT DIFFERENT SCALES

Figure 6. MODELED ROUGH SURFACE: CONICAL ASPERITIES AT DIFFERTENT LEVELS

The general shape of surface asperities is assumed to be a cone. Each cone (asperity) is covered with a smaller-size set of cones (another roughness level). By adding several levels of roughness, a fractal-type model of rough surfaces is built. As schematically shown in Fig. 6, the height and base radius of cones are different depending on the roughness level. To maintain a self-similarity, the side angle θ is assumed to be the same for all levels of roughness. It should be noted that the modeled rough surface covers both valleys and hills on a rough surface since concave cone (presenting hills) and convex cone (presenting valleys) have identical surface area.

The lateral surface area of the first cone is, $A_0 = \pi (h_0/m)^2 \sqrt{1 + m^2}$ where $m = \tan \theta$. The projected area (the base area) is $A_{p,0} = \pi (h_0/m)^2$, thus the enhancement

5

of surface area due to the first level of roughness is:

$$A_0^* = \frac{A_0}{A_{p,0}} = \sqrt{1+m^2} \qquad (13)$$

The second set of cones are of base radius r_1 and of height h_1 with the same side angle θ. The lateral area of each of the second level cones is, $dA_1 = \pi\,(h_1/m)^2\,\sqrt{1+m^2}$, and the projected area for each second-level cone is, $dA_{p,1} = \pi\,(h_1/m)^2$. It is interesting to see that the ratio of $dA_1/dA_{p,1} = \sqrt{1+m^2}$ is the same as for the first level. Assuming the surface area of the first cone is completely covered with cones, the number of the second level cones can be found:

$$N_1 = \frac{A_0}{dA_{p,1}} = \left(\frac{h_0}{h_1}\right)^2 \sqrt{1+m^2} \qquad (14)$$

The real surface area with two roughness levels is

$$A_1 = A_0 + N_1\, dA_{p,1}\left(\frac{dA_1}{dA_{p,1}} - 1\right) \qquad (15)$$

After substitution and simplification, one finds that $A_1^* = A_1/A_0 = \sqrt{1+m^2}$. Following the same steps, it can be shown that

$$\frac{A_{n+1}}{A_n} = \sqrt{1+m^2} \qquad (16)$$

Therefore, the increase in real surface area due to roughness where n scales (levels) of roughness is considered becomes:

$$A^* = \frac{A}{A_0} = \left(1+m^2\right)^{n/2} \qquad (17)$$

A relationship similar to Eq. (17) can be derived for the length ratio $\left[l^* = l/l_0 = \left(1+m^2\right)^{n/2}\right]$ of the one-dimensional fractal geometries shown in Fig. 5. This is in agreement with the isotropic roughness assumption, i.e., each trace of roughness measurement contains all the roughness characteristics of a Gaussian surface.

The surface slope m is also a random parameter with a Gaussian distribution:

$$\phi\,(m) = \frac{1}{\sqrt{2\pi}\sigma_m}\exp\left(-\frac{m^2}{2\,\sigma_m^2}\right) \qquad (18)$$

where σ_m is the surface slope standard deviation, see Eq. (5). To account for this variation of surface slope, Eq. (17) is weighted with the Gaussian distribution. Thus, the statistical effective real surface area can be found from:

$$A^* = \frac{A}{A_0} = \int_{-\infty}^{+\infty} \left(1+m^2\right)^{n/2} \phi\,(m)\,\,dm \qquad (19)$$

Equation (19) should be solved numerically. Figure 7 and Table 1 present the effect of roughness on real surface area
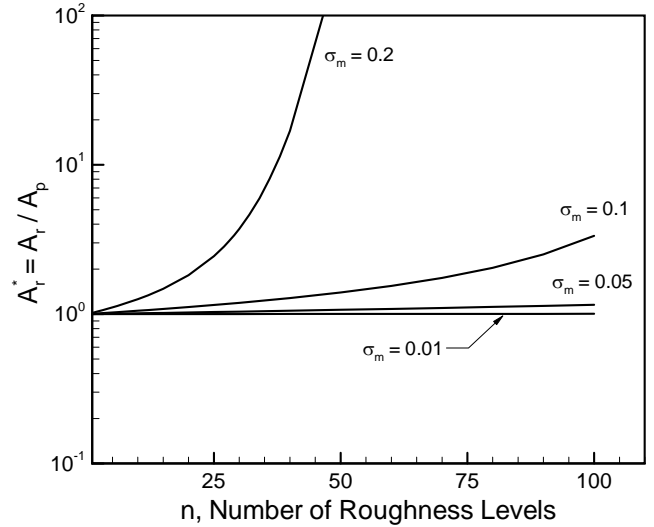

Figure 7. SURFACE AREA AS SCALE NUMBER AND SURFACE SLOPE ARE VARIED

A^* for four different levels of surface slope standard deviations $\sigma_m = 0.01$, 0.05, 0.1, and 0.2. As expected, by increasing the number of roughness levels n, the real surface area is increased (without a limit when $n \to \infty$). Moreover, the increase in real area is higher for surfaces with larger surface slopes.

Table 1. INCREASE IN SURFACE AREA AS SCALE NUMBER AND SURFACE SLOPE ARE VARIED

$\sigma_m =$	0.01	0.05	0.1	0.2
n	$A^* = A/A_0$			
1	1.0001	1.0013	1.0050	1.0190
2	1.0001	1.0025	1.0100	1.0400
3	1.0002	1.0037	1.0150	1.0617
4	1.0002	1.0050	1.0200	1.0850
5	1.0003	1.0063	1.0260	1.1093
6	1.0003	1.0076	1.0310	1.1354
10	1.0005	1.0127	1.0531	1.2590
12	1.0006	1.0153	1.0648	1.3358
15	1.0008	1.0190	1.0830	1.4775
20	1.0010	1.0260	1.1155	1.8243
25	1.0013	1.0330	1.1511	2.4410
30	1.0015	1.0396	1.1901	3.7161
40	1.0020	1.0540	1.2812	16.860
50	1.0025	1.0688	1.3956	258.59

Notice that at the limit where roughness goes to zero $\epsilon \to 0$ (smooth surface), $A^* \to 1$. The number of roughness levels, n, should be estimated when compared against experimental data. Also it can be seen that the surface en-
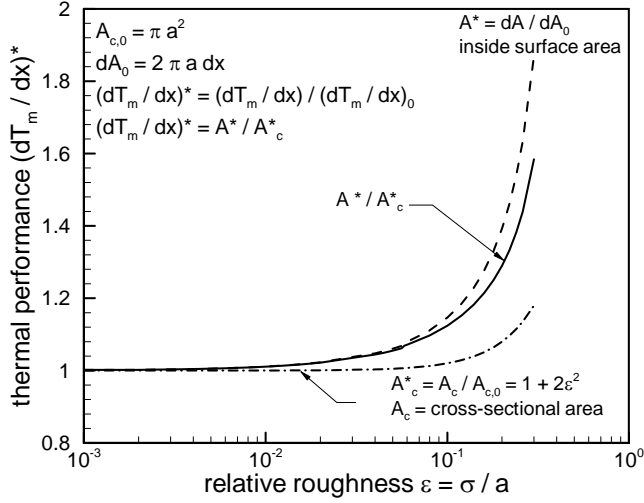
Figure 8. EFFECT OF ROUGHNESS ON THERMAL PERFORMANCE OF A MICROTUBE

hancement A^* is not sensitive to the number of roughness levels, n.

4.3 Effect of Roughness on Thermal Performance

Substituting Eqs. (12) and (19) into Eq. (1), the thermal performance becomes:

$$\frac{dT_m}{dx} = \frac{2q_w \, A^*}{\rho \, c_p a \, u_m \, (1 + \epsilon^2)} \tag{20}$$

Assuming a constant wall heat flux q_w and a constant mean velocity u_m as roughness is varied, the effect of roughness on thermal performance of microtubes can be determined. Figure 8 illustrates the effect of roughness on the thermal performance of a microtube where:

$$\left(\frac{dT_m}{dx}\right)^* = \frac{(dT_m/dx)}{(dT_m/dx)_0} = \frac{A^*}{1 + 2\epsilon^2} \tag{21}$$

Figure 8 shows an increase in the thermal performance due to introducing wall roughness. Recent advances in MEMS fabrication techniques allow several manufacturing methods that can be utilized to fabricate periodic surfaces. The present model can be used to predict an optimize design for the thermal performance of periodic microtubes/microchannels with or without roughness. It should be noted that as wall roughness increases, the pressure drop in microtubes also increases, see [8] for more detail. Therefore, both pressure drop and thermal performance should be considered in the optimizing procedure when designing microtubes.

To estimate the surface slope, the following empirical relationship is used [21]:

$$m_{abs} = 0.076 \, \sigma^{0.52} \tag{22}$$

The uncertainty of the above correlation is high, and use of this correlation is justifiable only where the surface slope is not reported and/or a rough estimation of m_{abs} is needed [22]. Also, an arbitrary value for the number of roughness levels n is considered.

5 ROUGHNESS AND NUSSELT NUMBER

Consider a fluid passing through a microtube where its temperature is changing as a result of heat transfer with the microtube wall. From Fourier's law:

$$q_w = -k\frac{\partial T}{\partial r}\bigg|_{wall} \tag{23}$$

Defining a non-dimensional temperature [13]:

$$\theta_T = \frac{T_s - T}{T_s - T_m} \tag{24}$$

Also $\eta = r/a$. Using the definition of the convective heat transfer coefficient, $q_w = h\,(T_s - T_m)$, Eq. (23) becomes:

$$Nu = 2\,\frac{\partial \theta_T}{\partial \eta}\bigg|_{wall} \tag{25}$$

where $Nu = hD/k$ is the local Nusselt number and $D = 2a$. As shown in Eq. (25), Nusselt number is twice the derivative of the non-dimensional temperature profile at the wall, see Fig. 9.

The wall roughness is assumed to be small compared to the tube radius. It is also assumed that the fluid flow remains laminar. This assumption is justifiable for low Reynolds numbers where inertial forces are small relative to viscous forces. Therefore, the non-dimensional temperature profiles remain unchanged as roughness is introduced. Thus, Nusselt number is not a function of wall roughness, see Eq. (25). In other words, since the slope of the non-dimensional temperature profile at the wall is independent of the tube local radius, Nusselt number will not change as the local radius varies due to roughness, see Fig. 9. This amounts to neglecting the possible effects of contraction/expansion of the fluid flow on heat transfer. Since the surface slopes of random rough surfaces are quit small (in the order of few degrees), this should not introduce a significant error.

Using Eq. (8) a relationship can be found for the convective heat transfer coefficient h

$$h = \frac{kNu}{2} \int_{-\infty}^{+\infty} \int_{-\infty}^{+\infty} \frac{\phi\,(p)\,\phi\,(q)}{(a + p + q)}dp\,dq \tag{26}$$
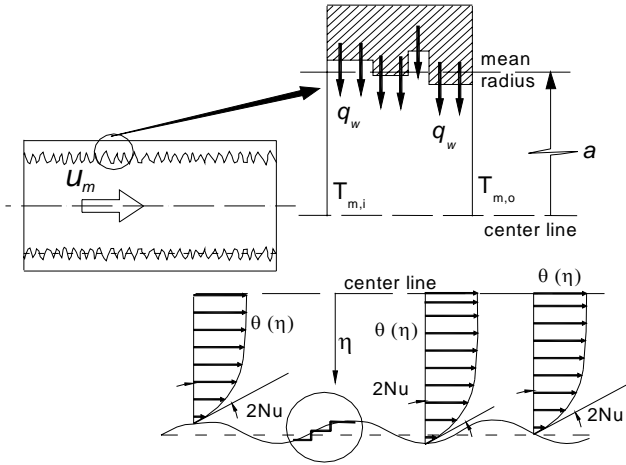
Figure 9. NON-DIMENSIONAL TEMPERATURE PROFILE IS NOT A FUNCTION OF LOCAL RADIUS

Figure 10. EFFECT OF ROUGHNESS ON CONVECTIVE HEAT TRANSFER COEFFICIENT

where $\phi(p)$ and $\phi(q)$ are defined in Eqs. (6) and (7), respectively.

The effect of roughness on the convective heat transfer can be presented as a correction factor with respect to smooth microtubes:

$$h^* = \frac{h}{h_0} = \frac{1}{2\pi} \int_{-\infty}^{+\infty} \int_{-\infty}^{+\infty} \frac{e^{-u^2/2} e^{-v^2/2}}{1 + \epsilon(u+v)} du\, dv \qquad (27)$$

where $h_0 = kNu/2a$ is the convective heat transfer coefficient for smooth microtubes. Equation (27) is solved numerically and the results are curve-fitted. The following correlation can be used to find h^*:

$$h^* = \frac{h}{h_0} = \frac{1}{1 - 1.38\,\epsilon^{1.785}} \qquad (28)$$

Figure 10 shows the effect of roughness on the convective heat transfer coefficient. As shown, the effect of roughness on h is quite small and can be neglected for most applications.

6 SUMMARY AND CONCLUSIONS

The effect of random, isotropic surface roughness on convective heat transfer in laminar, single-phase flow in rough microtubes is studied and a novel analytical model is developed. A new parameter, change in the fluid mean temperature over the tube length, is defined as a figure of merit to assess the thermal performance of randomly rough microtubes.

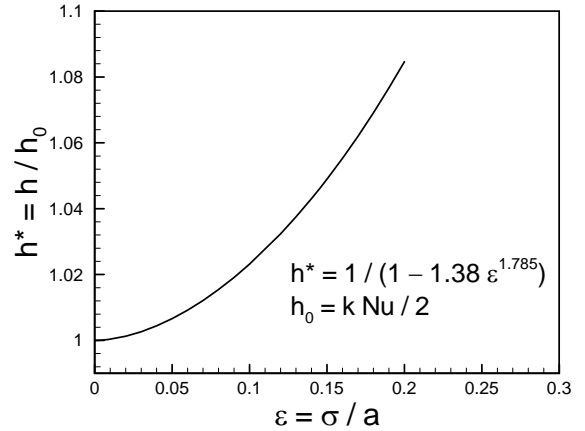The results for cylindrical rough microchannels are presented; however, the proposed model can be extended to other geometries such as rectangular and trapezoidal microchannels. As a result of advances in fabrication techniques of MEMS, many processing techniques can be utilized to fabricate periodic surfaces. The present model can be implemented to optimize the thermal performance of periodic surfaces with or without roughness.

Two independent random variables are considered to account for deviations of the local radius of rough microtubes in the angular and longitudinal directions. The local radius is assumed to be the superposition of the two random variables. Relationships are derived for the cross-sectional area and the convective heat transfer coefficient of randomly rough microtubes.

Using fractal concepts, a new statistical model is developed for estimating the real surface area of random rough surfaces. The general shape of surface asperities is assumed conical. The following are found through analysis:

- as a result of roughness, both cross-sectional and surface area of microtubes are increased
- the thermal performance of microtubes increases by increasing wall roughness. This increase comes at the expense of a higher pressure drop
- Nusselt number remains unchanged as wall roughness is introduced
- the convective heat transfer coefficient slightly increases by increasing wall roughness; however, this increase is relatively small and may be ignored for most applications.

A relatively large scatter is observed in the published heat transfer data. Therefore, the model is not compared with the data. Performing careful experimental investigation is highly recommended to validate the present model.

Copyright © 2005 by ASME

However, it should be mentioned that designing and conducting such experiments is a great challenge due to the small size of microtubes. Further, the present model requires a parameter, the roughness scale number n, which should be estimated from the comparison with experimental result.

REFERENCES
[1] Morini, G. L., 2004. "Single-phase convective heat transfer in microchannels: A review of experimental results". *Int. J Thermal Sciences,* **43** , pp. 631–651.

[2] Duncan, A. B., and Peterson, G. P., 1994. "Review of microscale heat transfer". *Journal of Applied Mechanics Review,* **47** , pp. 397–428.

[3] Papautsky, I., and Ameel, T., 2001. "A review of laminar single-phase flow in microchannels". *ASME, Proceedings of Int. Mech. Eng Congress Expos Proc (IMECE) 2001, ASME, New York,* **2** , pp. 3067–3075.

[4] Sobhan, C. B., and Garimella, S. V., 2001. "A comparative analysis of studies on heat transfer and fluid flow in microchannels". Microscale Thermophysical Engineering, **5** (4) , pp. 293–311.

[5] Li, Z., Du, D., and Guo, Z., 2003. "Experimental study on flow characteristics of liquid in circular microtubes". Microscale Thermophysical Engineering, **7** (3) , pp. 253–265.

[6] Judy, J., Maynes, D., and Webb, B. W., 2002. "Characterization of frictional pressure drop for liquid flows through microchannels". *Int. J Heat Mass Transfer,* **45** , pp. 3477–3489.

[7] Wu, H. Y., and Cheng, P., 2003. "An experimental study of convective heat transfer in silicon microchannels with different surface conditions". *Int. J Heat Mass Transfer,* **46** , pp. 2547–2556.

[8] Bahrami, M., Yovanovich, M. M., and Culham, J. R., 2005. "Pressure drop of fully developed, laminar flow in rough microtubes". *ASME 3rd International Conference on Microchannels, July 13-15, U. of Toronto, Canada* .

[9] Celata, G., Cumo, M., and Zummo, G., 2004. "Thermal-hydraulic characteristics of single-phase flow in capillary pipes". *Experimental Thermal and Fluid Science,* **28** , pp. 87–95.

[10] Kandlikar, S. G., Joshi, S., and Tian, S., 2001. "Effect of channel roughness on heat transfer and fluid flow characteristics at low reynolds numbers in small diameter tubes". *Proceedings of the National Heat Transfer Conference, ASME,* **2** , pp. 1609–1618.

[11] Gao, P., Person, S. L., and Favre-Marinet, M., 2002. "Scale effects on hydrodynamics and heat transfer in two-dimensional mini and microchannels". *Int. J Thermal Sciences,* **41** , pp. 1017–1027.

[12] Obot, N. T., 2002. "Toward a better understanding of friction and heat/mass transfer in microchannels- a literature review". *Microscale Thermophysical Engineering,* **6** , pp. 155–173.

[13] Kays, W. M., and Crawford, M. E., 1980. *Convective Heat and Mass Transfer.* McGraw-Hill, New York.

[14] Liu, G., Wang, Q., and Ling, C., 1999. "A survey of current models for simulating contact between rough surfaces". Tribology Trans., **42** (3) , pp. 581–591.

[15] Johnson, K. L., 1985. *Contact Mechanics.* Cambridge University Press, Cambridge, UK, ch. 13.

[16] Ling, F. F., 1958. "On asperity distributions of metalic surfaces". Journal of Applied Physics, **29** (8) .

[17] Mikic, B. B., and Rohsenow, W. M., 1966. Thermal contact conductance. Tech. rep., Dept. of Mech. Eng. MIT, Cambridge, Massachusetts, NASA Contract No. NGR 22-009-065, September.

[18] Majumdar, A., and Tien, T. L., 1991. "Fractal characterization and simulation of rough surfaces". *Journal of Tribology,* **113** , pp. 1–11.

[19] Majumdar, A., and Bhushan, B., 1990. "Fractal model of elastic-plastic contact between rough surfaces". *Wear,* **136** , pp. 313–327.

[20] Mandelbrot, B. B., 1977. *The Fractal Geometry of Nature.* W. H. Freeman and Company, New York, NY, U.S.A.

[21] Lambert, M. A., and Fletcher, L. S., 1997. "Thermal contact conductance of spherical rough metals". Journal of Heat Transfer, ASME, **119** (4) , pp. 684–690.

[22] Bahrami, M., Culham, J. R., Yovanovich, M. M., and Schneider, G. E., 2004. "Review of thermal joint resistance models for non-conforming rough surfaces in a vacuum". *ASME Journal of Applied Mechanics, in press, also HT2003-47051* .